Encapsulation of hydrophobic components in dendrimersomes and decoration of their surface with proteins and nucleic acids

Paola Torre[a], Qi Xiao[b,c], Irene Buzzacchera[b,d,e], Samuel E. Sherman[b], Khosrow Rahimi[d,f], Nina Yu. Kostina[d,f], Cesar Rodriguez-Emmenegger[d,f], Martin Möller[d,f], Christopher J. Wilson[e], Michael L. Klein[c,1], Matthew C. Good[a,g,1], and Virgil Percec[b,1]

[a]Department of Cell and Developmental Biology, Perelman School of Medicine, University of Pennsylvania, Philadelphia, PA 19104-6058; [b]Roy & Diana Vagelos Laboratories, Department of Chemistry, University of Pennsylvania, Philadelphia, PA 19104-6323; [c]Institute of Computational Molecular Science, Temple University, Philadelphia, PA 19122; [d]DWI–Leibniz Institute for Interactive Materials, 52074 Aachen, Germany; [e]NovioSense B.V., 6534 AT Nijmegen, The Netherlands; [f]Institute of Technical and Macromolecular Chemistry, RWTH Aachen University, 52074 Aachen, Germany; and [g]Department of Bioengineering, University of Pennsylvania, Philadelphia, PA 19104-6321

Contributed by Michael L. Klein, June 11, 2019 (sent for review March 21, 2019; reviewed by Juliane Nguyen and Ling Peng)

Reconstructing the functions of living cells using nonnatural components is one of the great challenges of natural sciences. Compartmentalization, encapsulation, and surface decoration of globular assemblies, known as vesicles, represent key early steps in the reconstitution of synthetic cells. Here we report that vesicles self-assembled from amphiphilic Janus dendrimers, called dendrimersomes, encapsulate high concentrations of hydrophobic components and do so more efficiently than commercially available stealth liposomes assembled from phospholipid components. Multilayer onion-like dendrimersomes demonstrate a particularly high capacity for loading low-molecular weight compounds and even folded proteins. Coassembly of amphiphilic Janus dendrimers with metal-chelating ligands conjugated to amphiphilic Janus dendrimers generates dendrimersomes that selectively display folded proteins on their periphery in an oriented manner. A modular strategy for tethering nucleic acids to the surface of dendrimersomes is also demonstrated. These findings augment the functional capabilities of dendrimersomes to serve as versatile biological membrane mimics.

Janus dendrimer vesicles | onion-like vesicles | biological membrane mimic | folded protein | nucleic acid

Compartmentalization by self-assembly of lipids is a key element to the origin of life (1, 2), contributing to the organization of cellular membranes, the only common element of most organisms of life (1, 3–5). Natural membranes achieve an incredibly rich functionality by the self-assembly of few building blocks, mainly phospholipids and proteins but also functional elements such as transmembrane proteins, sphingolipids, etc. (1, 6–8). Remarkably, their functionality goes beyond the collection of its elements resulting in complex 2D segregation into microdomains (rafts) and nanodomains with synergistic functions (9, 10) combined with exquisite control of the mechanical properties of the membrane.

In the last decade, researchers endeavored to develop synthetic cells that can mimic functions known from living cells to study fundamental aspects of living systems (3, 4, 11–13). Giant unilamellar and multilamellar vesicles represent a promising and extremely useful biomembrane model system that provides access for systematic studies of mechanical, thermodynamic, electrical, and rheological properties as well as to introduce chemical and biological function (10, 14). Liposomes are lipid bilayer membranes formed from natural and synthetic lipids that accurately mimic the thickness, flexibility, and 2D dynamics of natural membranes (1, 15, 16). Nonetheless, they lack stability to environmental conditions, severely limiting their use for advance functions (7, 17). Stealth liposomes are stable vesicles containing a mixture of phospholipids, phospholipid conjugated with poly(ethyleneglycol) (PEG), and cholesterol (18).

Polymersomes assembled from amphiphilic block copolymers have received considerable attention (19, 20). Although they have sufficient stability, the thickness of the polymersome membrane is larger than that of the cell membranes, and the component copolymers lack the lateral mobility of lipids in cells, which causes different mechanical and dynamic behavior. Moreover, the inherent polydispersity of synthetic macromolecules affects the reproducibility of the assembly process.

Amphiphilic Janus dendrimers and glycodendrimers provide alternatives to lipids capable of self-assembly into vesicles and display special characteristics, such as enhanced stability, compared with liposomes in vitro (21–26). Their perfectly monodisperse structure can be tuned to generate cell membranes with the same thickness, flexibility, and mechanical resistance as natural cells. The higher stability of dendrimersomes is the result of additional weak intermolecular forces such as π–π interactions between aromatic branching centers in dendrons in addition to

Significance

Lipid vesicles are globular assemblies that compartmentalize, encapsulate, transport, and provide signal transmission and communication between cells. In living systems, these vesicles perform critical functions to sustain life. Biomimetic lipid vesicles, such as liposomes, have been developed as mimics of biological cell membranes and for applications in biotechnology, but they do have specific limitations. Dendrimersomes are vesicles self-assembled from amphiphilic Janus dendrimers. They offer improved stability and versatility over liposomes. These dendrimersomes are extremely efficient at loading hydrophobic small molecules and natural macromolecules including folded proteins, at a level higher than comparable liposomes. Additionally, they can be readily functionalized to enable modular recruitment of proteins and nucleic acids on their periphery.

Author contributions: P.T., Q.X., M.L.K., M.C.G., and V.P. designed research; P.T., Q.X., I.B., S.E.S., K.R., N.Y.K., and C.R.-E. performed research; P.T., Q.X., C.R.-E., M.L.K., M.C.G., and V.P. analyzed data; M.M. and C.J.W. contributed new reagents/analytic tools; and P.T., Q.X., C.R.-E., M.L.K., M.C.G., and V.P. wrote the paper.

Reviewers: J.N., University of North Carolina at Chapel Hill; and L.P., Aix-Marseille Université and CNRS.

The authors declare no conflict of interest.

[1]To whom correspondence may be addressed. Email: mlklein@temple.edu, mattgood@pennmedicine.upenn.edu, or percec@sas.upenn.edu.

This article contains supporting information online at www.pnas.org/lookup/suppl/doi:10.1073/pnas.1904868116/-/DCSupplemental.

Published online July 15, 2019.

hydrophobic interactions and a larger number of hydrophobic chains per molecule, which reduces the critical assembly concentration (27). These amphiphilic Janus dendrimers can also be conjugated with sugars and assembled into glycodendrimersomes that mimic the glycans on biological membranes (21, 28–34). Additionally, they can be transformed into cell-like hybrids with either bacterial (24) or human cells (25). As with cell membranes, the bilayers of these supramolecular constructs act as a barrier between the inside and outside of dendrimersomes, glycodendrimersomes, and cell-like hybrids (21–25). Selective permeation can be provided, with comparable efficiency as with liposomes (35) and polymersomes (36), when either pore-forming transmembrane proteins or their mimics are incorporated into the bilayer (24, 25). Recently, the assembly of bicomponent dendrimers, dendrons with oligoethylene oxide and lactose, resulted in the formation of nanodomains, which represent a synthetic example of membrane nanoparterning that underpins the basis of primitive cell communication (34). Such domains have been observed on natural cells and recently in modulated phase patterns in quaternary mixture of phospholipids as a consequence of competing line tension due to the hydrophobic mismatch and local curvature (10, 14). Therefore, dendrimersomes and glycodendrimersomes function as biological membrane mimics that can help to elucidate concepts in synthetic cell biology and glycobiology such as compartmentalization, encapsulation and release, and selective transport (21–25), as well as fusion and fission (37, 38).

Currently, it has been a challenge to decorate the periphery of dendrimersomes with proteins and nucleic acids to add further levels of interaction with natural cells. Here the higher stability of dendrimersomes allows for the introduction of functionality beyond what can be achieved with liposomes. Specifically, higher amounts of hydrophobic molecules can be loaded into the membrane compared with liposomes. In addition, a nitrilotriacetic acid (NTA)-conjugated dendrimer was introduced to functionalize the periphery of the dendrimersomes via bioaffinity interactions. Such an approach does not pose any pressure on the stability of the dendrimersome and maintains the high lateral mobility for advanced functions. In addition, given the large number of recombinant proteins tagged with histidine, this approach is versatile. Thus, a large number of functional proteins and nucleic acids can be used to decorate the periphery of dendrimersomes to enrich functional behavior without modifying the basic dendrimersome platform.

Results and Discussion

Higher Loading of Hydrophobic Molecules in Onion-Like Dendrimersomes Compared with Stealth Liposomes. Dendrimersomes were prepared by the self-assembly of amphiphilic Janus dendrimers in water. Giant (1–20 microns) unilamellar and onion-like vesicles (26, 37, 39) were prepared via thin-film rehydration to enable their characterization by optical microscopy.

The Janus dendrimers used in this study (Fig. 1) had been synthesized by previously reported methods, and their dendrimersomes have been characterized by cryogenic transmission electron microscopy (22, 37, 39, 40).

To evaluate the capabilities of these dendrimersomes, their efficiency at loading low-molecular weight dyes, drugs, and large cargos such as proteins and DNA was compared with the loading capability of commercial stealth liposomes (18). A standard thin-film hydration procedure that included 0.5 mol % of fluorescent Janus dendrimer (R_H-RhB, R_F-RhB, red) (Fig. 1) was used for imaging. The spontaneous loading of small molecules was evaluated during the hydration step. A hydrophobic dye, borondipyrromethene (BODIPY) (Fig. 2), which is excited at 488 nm, was first tested. Compared with unilamellar stealth liposomes, unilamellar dendrimersomes loaded significantly higher concentrations of hydrophobic dye (Fig. 2 *A*–*C*). For both types of vesicles, the hydrophobic dye appeared to concentrate in the lamellar layer likely due to a combination of hydrophobic interactions and interactions of the π system of BODIPY and of aryl groups of the hydrophobic dendrons (Fig. 2*B*). The larger loading of hydrophobic molecules compared with the liposomes is a consequence of the higher stability of dendrimersomes (i.e., they can load more hydrophobic molecules before destabilization and due to the additional weak interactions described above). Therefore, the onion-like dendrimersomes, which offer a large number of lamellae in the same volume as a unilamellar object, are arguably ideal carriers for small hydrophobic molecules that fit in the bilayer. Indeed, it was found that onion-like dendrimersomes loaded between 5 and 15 times more dye than standard unilamellar liposomes (Fig. 2*C*). This is a significant finding because of the challenges associated with spontaneous loading of hydrophobic or neutrally charged molecules into liposome systems that aside from biological cell mimics are of interest also for medicine, cosmetics, and agriculture (41).

To evaluate the capability of dendrimersomes for enhanced loading of a hydrophobic drug, a basic form of the anthracycline drug Doxorubicin, which is used to treat solid tumors in various forms of cancer (42–44), was tested. Higher loading of Doxorubicin in both R_H-10 and R_F onion-like dendrimersomes compared with stealth liposomes was found (Fig. 2 *F* and *G*). These results confirm the general principle that hydrophobic small molecules can be loaded at elevated levels into multilamellar dendrimersomes (Fig. 2*H*). In all cases, onion-like dendrimers contained higher concentrations of the hydrophobic small molecules, BODIPY or Doxorubicin (Fig. 2 *C* and *G*), and demonstrated that elevated loading is likely due to association of the small molecule with the vesicle lamellae. A water-soluble amphiphilic

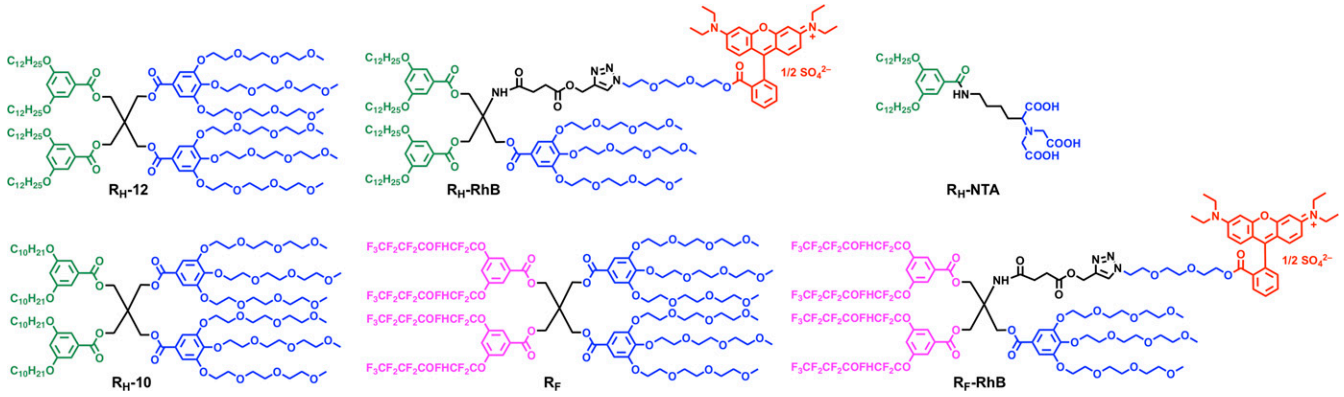

Fig. 1. Chemical structures of amphiphilic Janus dendrimers used for vesicle assembly, fluorescent labeling, and chelating.

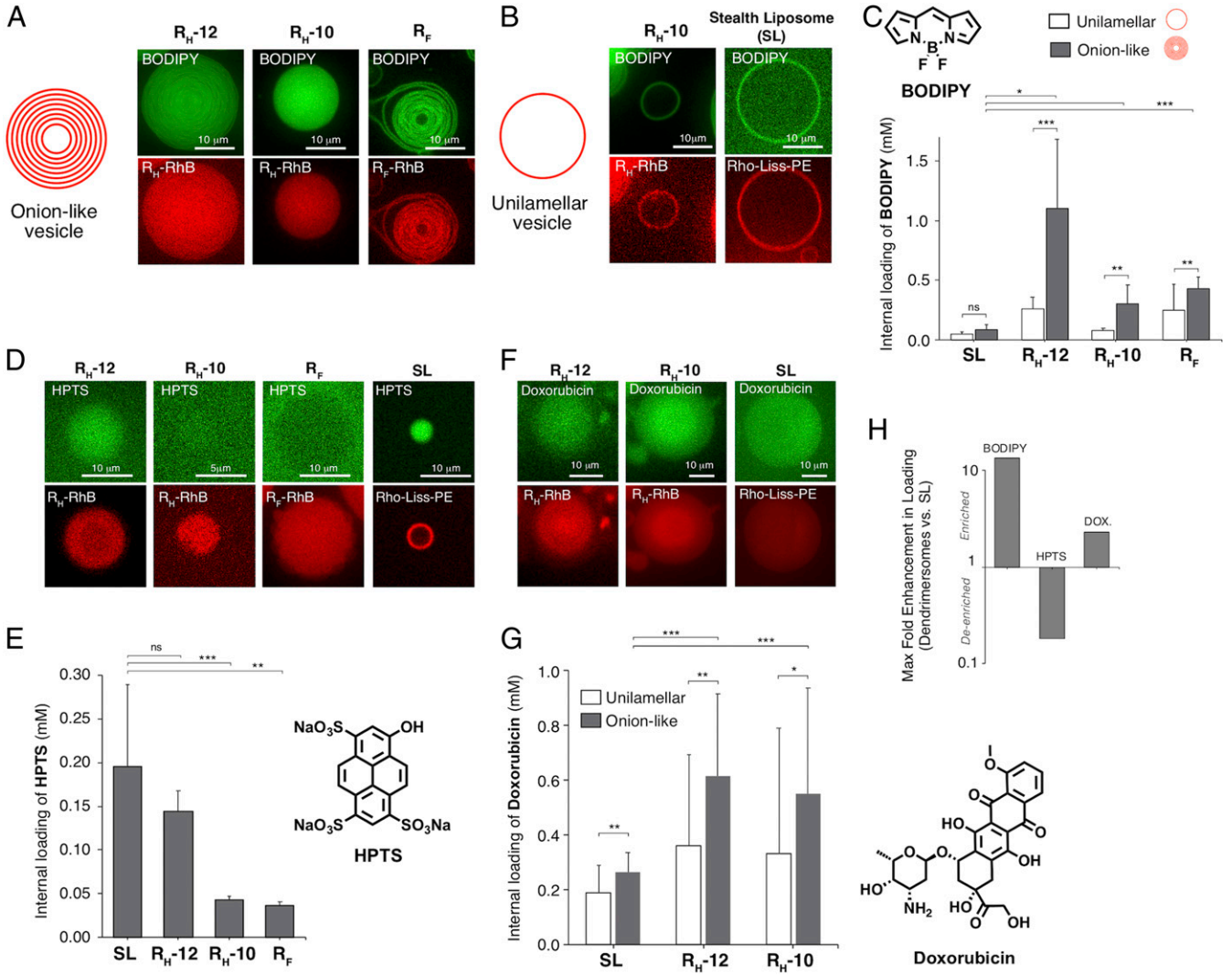

Fig. 2. Enhanced loading of hydrophobic small molecules in onion-like dendrimersomes. (*A*–*C*) Superior loading of hydrophobic small molecule, BODIPY, into dendrimersome vesicles compared with stealth liposomes. All vesicles formed by hydration. Onion-like dendrimersome vesicles load significantly higher concentrations of cargo than unilamellar vesicles. Representative confocal images of (*A*) multilamellar vesicles, and (*B*) unilamellar vesicles. (*C*) Image quantitation: R_H-12 dendrimersomes load >10-fold higher concentration of BODIPY cargo relative to either form of stealth liposome. (*D* and *E*) A hydrophilic small molecule, HPTS, loads more efficiently into stealth liposomes than dendrimersome vesicles; it is largely excluded from R_H-10 and R_F dendrimersomes. (*F* and *G*) Chemotherapeutic drug, doxorubicin, loads much more efficiently in R_H-10 dendrimersome onion-like vesicles compared with stealth liposomes. (*H*) Summary of max fold enhancement in small molecule loading, comparing dendrimersome to stealth liposome. Mean ± SD. *$P < 0.05$, **$P < 0.01$, and ***$P < 0.001$; ns, nonsignificant.

molecule, HPTS (Fig. 2*E*), displayed reduced rather than enhanced loading into dendrimersomes. In fact, this molecule was largely excluded from R_H-10 and R_F dendrimersomes and in all cases showed higher loading in stealth liposomes (Fig. 2 *D* and *E*). Exclusion from R_F might be connected with the incompatibility with the perfluorinated lamellae.

Superior Retention of Cargos within Dendrimersomes. To evaluate ability of vesicles to retain cargos under physiological conditions, we characterized the stability of dendrimersomes and of stealth liposomes at 37 °C in the presence of buffer containing 10% of FBS (Fig. 3). After 2 h of incubation, stealth liposomes showed a near–2.5-fold drop in bound hydrophobic cargo. In contrast, R_H-12 dendrimersomes retained 83%, demonstrating not only their higher loading capacity but their enhanced retention of cargos.

Design and Synthesis of a Janus Dendrimer Conjugated to an NTA Ligand. To localize the immobilization to the surface of the dendrimersomes, a nitrilotriacetic acid (NTA)-conjugated Janus dendrimer (R_H-NTA) that binds tightly to 6-His–tagged proteins was designed and synthesized (Fig. 4*A*). NTA is a tetradentate ligand which can bind metal ions such as Ni^{2+} together with multiple histidine (His) residues from proteins (Fig. 4*B*) (45). From a commercially available N_6 carboxybenzyl (Cbz) protected lysine **2**, tribasic acid **3** was obtained via S_N2 reaction with 2-bromo acetic acid in NaOH aqueous solution, followed by Fischer esterification with methanol in the presence of *p*-toluenesulfonic acid (TsOH) and deprotection of Cbz group via hydrogenolysis with palladium on carbon (46). Intermediate **5** containing a free amino group was conjugated with 3, 5-didodecyoxyl benzoic acid **6** via 2-chloro-4,6-dimethoxy-1,3,5-triazine (CDMT) and *N*-methylmorpholine (NMM) in THF to obtain compound **7** (67% yield). After hydrolysis with KOH in tetrahydrofuran and ethanol mixture and acidification with HCl aqueous solution, the target Janus dendrimer R_H-NTA **8** was obtained in 86% yield. Furthermore, intermediate **2** can be synthesized via Cu^{2+} salt forming a complex

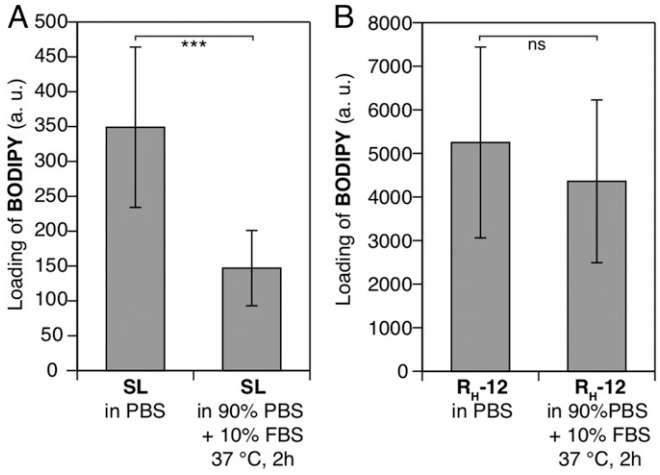

Fig. 3. Retention of hydrophobic cargo in vesicles and dendrimersomes. Amount of BODIPY loaded in (*A*) vesicles or (*B*) dendrimersomes before and after incubation with PBS + 10% FBS mixture at 37 °C for 2 h. Mean ± SD. ***$P < 0.001$; ns, nonsignificant; a.u., arbitrary units.

followed by CbzCl protection by using literature reaction conditions (47) when large-scale synthesis for the R_H-NTA is needed.

Encapsulation of Proteins into Dendrimersomes in the Absence and Presence of NTA Ligand. A major challenge for synthetic cell mimics is to add functionality to their periphery while maintaining their stability. In particular, to localize functional proteins or nucleic acids on the periphery is of upmost importance to achieve functions such as catalysis, division (48), and even locomotion. Here R_H-NTA (Fig. 4) was coassembled with Janus dendrimers R_H-12 or R_H-10. The resulting dendrimersomes have NTA groups in their inner and outer leaflets which were exploited for the bioaffinity immobilization of a His-tagged green fluorescent protein (GFP). GFP, having molecular weight of 25×10^3 g·mol^{-1}, 4 nm folded diameter, and acidic isoelectric point (pI), was selected as a representative of many proteins in bacteria and humans. This affinity immobilization enables one to place the biomacromolecule in any desired orientation, particularly important to enable maximum activity. (Fig. 5*A*). Spontaneous loading of His-GFP protein into onion-like liposomes and dendrimersomes without NTA (Fig. 5 *B* and *C*) was assessed by swelling the thin film of lipids or dendrimersomes in an aqueous solution of His-GFP. It was found that dendrimersomes were able to achieve more than 6-fold higher cargo loading than that achieved by stealth liposomes.

We assayed immobilization of 6-His-GFP protein to the surface of R_H-12 and R_H-10 dendrimersomes in the presence of R_H-NTA (Fig. 6). A control experiment with dendrimersomes that lacked NTA demonstrated that NTA-based dendrimersomes bound between a 10- to 100-fold higher amount of recruited protein at the vesicle outer membrane (Fig. 6*B*). Surface recruitment does not depend on the extent of lamellarity. These results demonstrate a general strategy for highly selective conjugation of His-tagged proteins to the surface of dendrimersome vesicles.

Modular Tethering of DNA to SNAP-Tagged Dendrimersomes. Decoration of the dendrimersome periphery with DNA is an important tool toward construction of synthetic cells. The hybridization of immobilized DNA can be exploited to induce binding, fusion, or fission or even to fix synthetic cells to surfaces as surrogates of stratified tissues. However, this experiment is challenging because the charge density of DNA imposes an osmotic pressure on the vesicle and can locally alter membrane curvature and morphology (49). To demonstrate the power of the NTA-dendrimersome platform for recruiting DNA, vesicles were decorated with His-SNAP, a protein that binds covalently to benzyl guanine (BG)

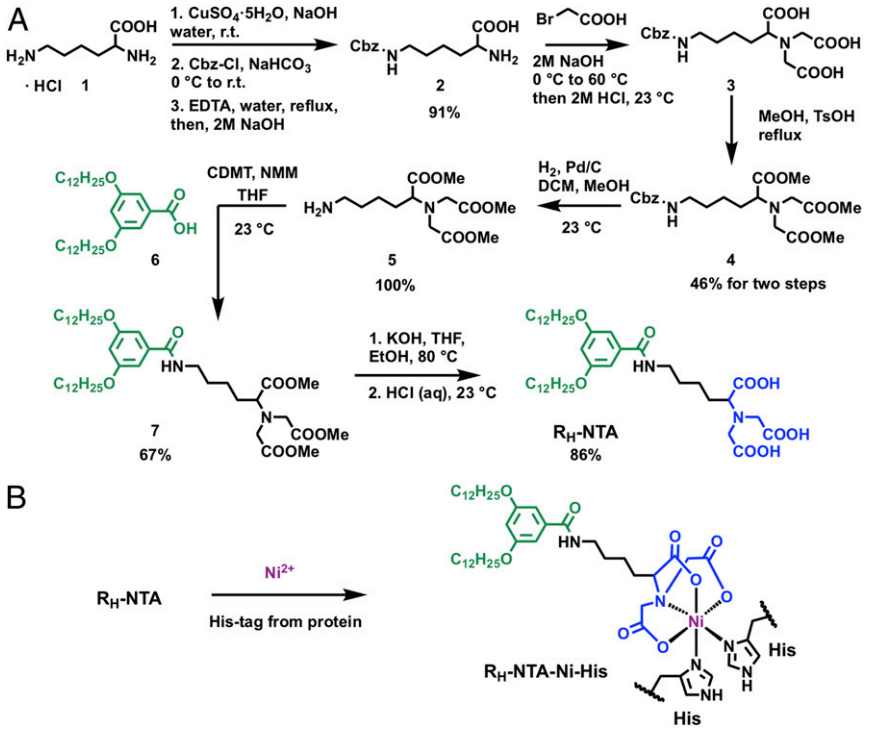

Fig. 4. (*A*) Synthesis of a Janus dendrimer conjugated to a nitrilotriacetic acid (NTA) ligand (R_H-NTA) and (*B*) scheme of R_H-NTA binding to histidine (His) residues from proteins.

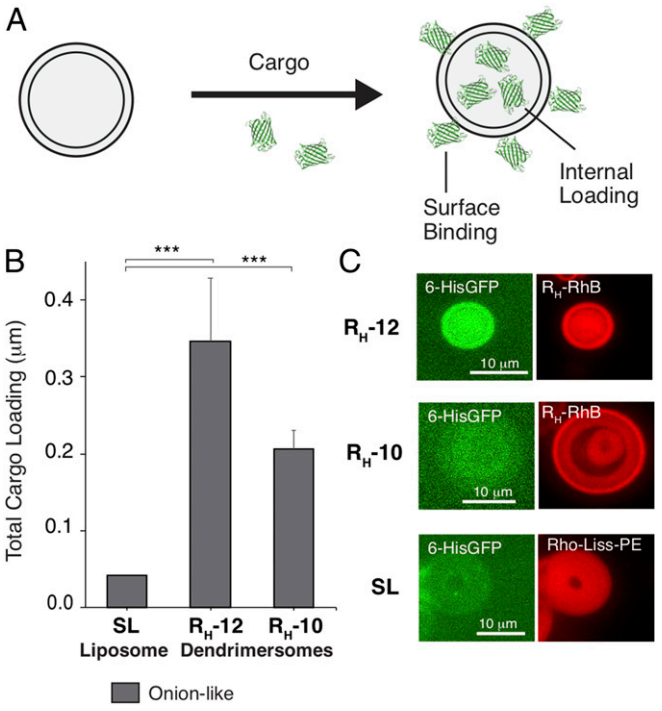

Fig. 5. Protein recruitment to dendrimersomes without NTA ligand. (*A*) Schematic of protein internal loading and surface binding to dendrimersome and liposome vesicles. (*B*) Dendrimersomes display higher spontaneous loading of protein cargos compared with stealth liposomes in their onion-like structures. (*C*) Confocal images show higher loading of His-GFP cargo to multilamellar dendrimersomes and stealth liposomes. Mean ± SD. ***$P < 0.001$.

(Fig. 7 *A* and *B*). This was exploited to bind DNA oligomers that were conjugated to BG to SNAP-decorated dendrimersomes. An ALC aptamer (EJ4), a DNA therapeutic that has been used for study and treatment of lung carcinomas, was selected for this experiment (50, 51). This 40+ nucleotide ssDNA molecule was also conjugated to a fluorescein amidite (FAM) dye to enable visualization by confocal fluorescence microscopy. The resulting dendrimersome vesicle contains both protein and DNA as layers and illustrates a general strategy to conjugate nucleotides to the outer periphery of vesicles (Fig. 7*C*). DNA aptamer was only strongly recruitment to liposomes and stealth liposomes that contained NTA dendrimer (Fig. 7 *D* and *E*). Nonspecific recruitment of DNA aptamer via SNAP protein was observed for dendrimersomes, which is consistent with the recruitment of proteins such as GFP to dendrimersomes in the absence of NTA ligand (Fig. 5). Nonetheless, recruitment to dendrimersomes was enhanced, particularly at the vesicle exterior, in the presence of NTA. Stealth liposomes and non-PEG conjugated liposome containing DGS-NTA lipid recruited the DNA aptamer to a lower extent to that of NTA dendrimersomes (Fig. 7*E*). The presence of PEG in the stealth liposomes does not interfere with binding of protein to NTA-containing liposomes (Fig. 7*E*).

Conclusions

The platform presented here offers a strategy to modularly tether bioactive cargos to the periphery of the membrane-mimetic dendrimersome. These cargos include proteins and nucleic acids, as well as the hydrophobic molecules of both low and high molecular weight. The loading achieved through thin-film hydration of dendrimersomes surpasses that which can be achieved by formulations of commonly employed stealth liposomes. Janus dendrimers can be readily functionalized with ligands, including NTA-conjugated Janus dendrimers, and incorporated into the lamellar structure of dendrimersomes to bind proteins containing tags common in molecular biology. For example, His-tagged SNAP protein enables subsequent covalent conjugation to BG-modified nucleic acids, such as therapeutic aptamers. This approach allows creation of versatile dendrimersome assemblies (52, 53) capable of binding to a broad range of nucleic acids, a

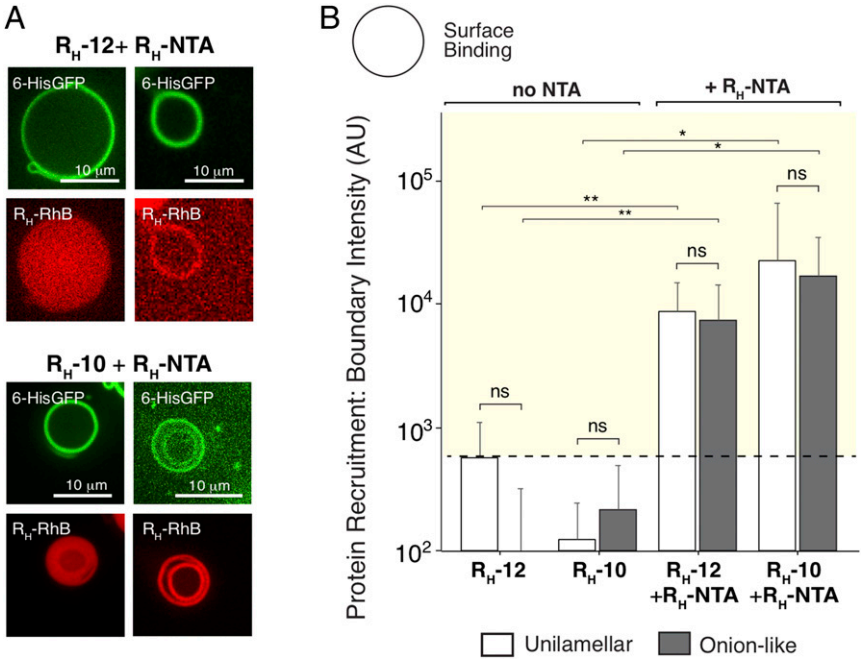

Fig. 6. Selective protein recruitment to dendrimersomes with NTA ligand. (*A*) Confocal images show selective recruitment of His-GFP to dendrimersomes containing R_H-NTA. (*B*) Quantitation of cargo recruitment to dendrimersomes: surface recruitment is specific to presence of R_H-NTA and does not depend on extent of lamellarity. Mean ± SD. *$P < 0.05$, **$P < 0.01$; ns, nonsignificant.

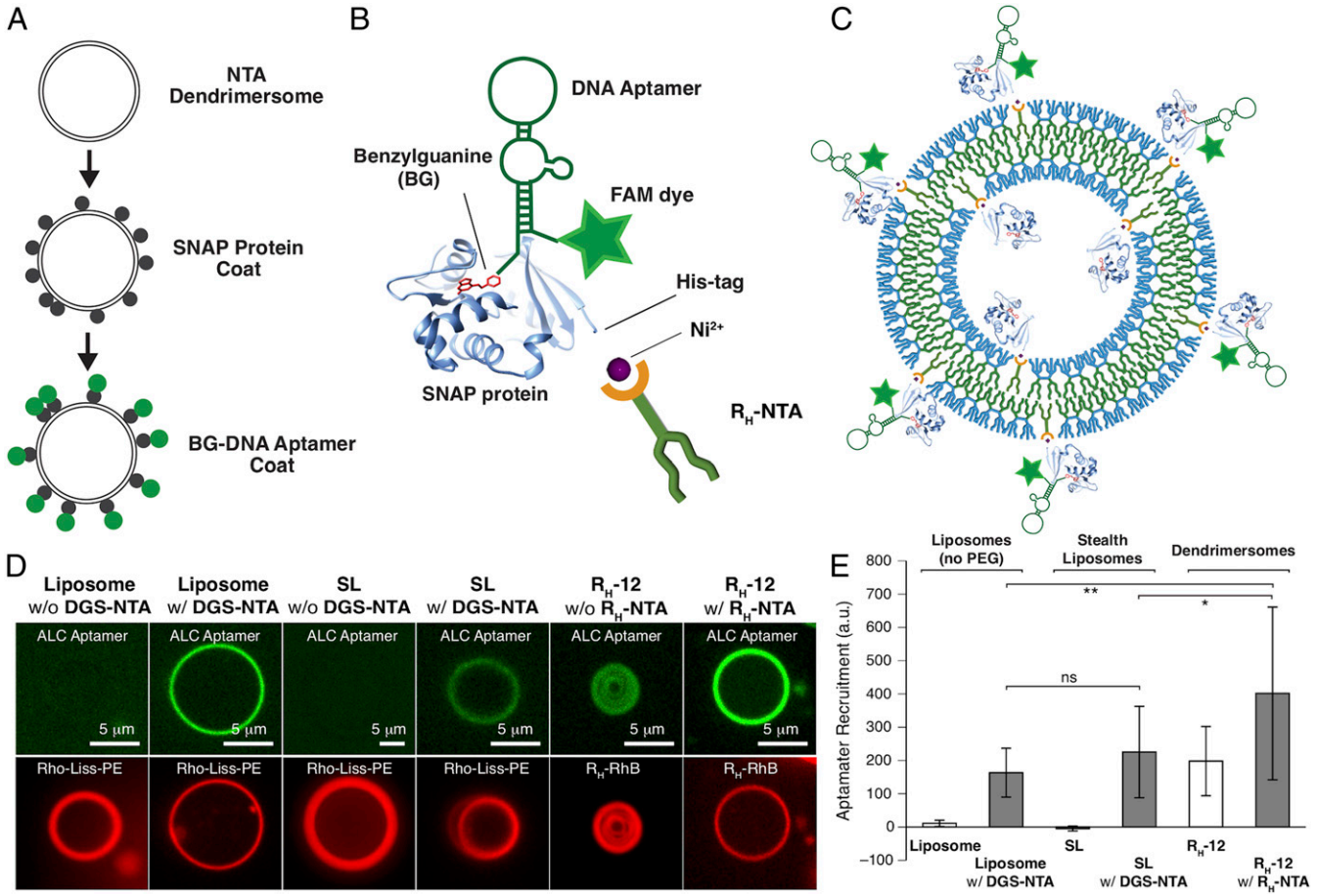

Fig. 7. Modular tethering of DNA to SNAP-tagged dendrimersomes. (*A*) Schematic showing layering of a protein and DNA coat to dendrimersome vesicle. (*B*) His-SNAP proteins binds to R_H-NTA to form the initial protein layer. SNAP binds to a BG conjugated to the DNA, allowing for modular formation of a second layer, composed of nucleic acids. The DNA aptamer is labeled with FAM to enable imaging. (*C*) Schematic of multilayer dendrimersome containing DNA and protein coat. (*D*) Binding of DNA aptamer to liposomes, stealth liposomes, or dendrimersome vesicles is dependent on presence of NTA group. (*E*) Quantitation of DNA aptamer recruitment to vesicle types. R_H-NTA dendrimersomes demonstrate elevated DNA recruitment compared with NTA liposomes. Mean ± SD. $*P < 0.05$, $**P < 0.01$; ns, nonsignificant.

useful characteristic for a variety of synthetic cell applications. The dendrimersome platform described herein offers (54, 55) a very efficient encapsulation of hydrophobic target compounds that broadens their previous utility as biological membrane mimics (34).

Methods

Molecular Biology, Proteins, and DNA. Plasmids for recombinant expression of His-GFP and His-SNAP were transformed into *Escherichia coli* Rosetta 2 cells (Novagen) for protein expression. Cultures were grown in LB at 37 °C to an OD_{600} of 0.4, then temperature shifted to 16 °C for 20 min and induced using 0.5 mM IPTG at an OD_{600} between 0.5 and 0.7. Cultures were grown overnight at 16 °C. Cells were harvested by centrifugation and resuspended in PBS. Cells were lysed with 3 cycles of sonication and freeze–thaw and clarified by centrifugation. The supernatants were incubated with Ni-NTA agarose superflow resin (Qiagen) for 1 h at 4 °C. After extensive washing, proteins were eluted in a buffer containing 150 mM NaCl, 25 mM Tris, 250 mM imidazole, pH 8, 10% glycerol, and then dialyzed overnight to remove imidazole.

DNA aptamer (GAA GAC GAG CGG CGA GTG TTA TTA CGC TTG GAA ACA ACC CC) was purchased from Integrated DNA Technologies and contained a 5′ BG and 3′ FAM fluorophore modifications. Fluorescent dyes, BODIPY-FL and 8-Hydroxypyrene-1,3,6-Trisulfonic Acid, Trisodium Salt or pyranine (HPTS) were purchased from ThermoFisher Scientific. HPLC purified doxorubicin hydrochloride was purchased from Sigma-Aldrich. BG-GLA-NHS for the functionalization of the 3′-amino aptamer was purchased from New England Biolabs.

Synthesis and Acquisition of Dendrimer and Lipid Molecules. The synthesis of Janus dendrimers is shown in *SI Appendix*.

Lipids. Hydrogenated soy phosphatidylcholine (HSPC), *N*-(carbonylmethoxyolyethylene glycol 2000)-1,2-distearoyl-*sn*-glycero-3-phosphoethanolamine sodium salt (mPEG-DSPE), 1,2-dioleoyl-*sn*-glycero-3-phosphoethanolamine-*N*-(lissamine rhodamine B sulfonyl) (ammonium salt) (18:1 Liss Rhod PE), and 1,2-dioleoyl-*sn*-glycero-3-[(*N*-(5-amino-1-carboxypentyl)iminodiacetic acid)succinyl] (ammonium salt) (DGS-NTA) were purchased as $CHCl_3$ solutions from Avanti Polar Lipids.

Preparation of Vesicles. Dendrimersomes and liposomes were prepared by thin-film hydration. A solution of dendrimers or lipids (2 mg/50 μL) in chloroform was deposited on a roughened Teflon sheet and dried under vacuum overnight to remove all of the solvent. For the preparation of the stealth liposomes a mixture of HSPC (4.45 mg), cholesterol (3.1 mg), and mPEG-DSPE (0.4 mg) and 18:1 Liss Rhod PE (0.001 mg, for imaging) were dissolved in 50 μL of chloroform. For the dendrimersome preparation, a solution of 2 mg/mL of R_H-10 or R_H-12 and 11 μg/mL of R_H-RhB (Rhodamine B labeled) in chloroform was prepared. This equated to a 99.4 mol % R_H-12 or R_H-10 and 0.5 mol % R_H-RhB. Mixtures with R_F dendrimer contained similar ratios of R_F-RhB. When present, R_H-NTA was used at 0.2 mg/mL, equating to 14.4 mol % of R_H-NTA. DGS-NTA lipid was used at 6 mol %.

After film formation and complete solvent evaporation, the films were rehydrated in 500 μL PBS (pH = 7.4, 0.5×) at 50 °C overnight.

Vesicle Loading of Small Molecules, Proteins, and DNA. When loading molecules into dendrimersome and liposome vesicles, BODIPY, Doxorubicin, and

HPTS were included during the hydration step at a final concentration of 1 mM. BODIPY was dissolved in DMSO and mixed in PBS before hydration of Janus dendrimer or lipid. Doxorubicin hydrochloride or HPTS was dissolved in PBS buffer (pH 7.4). Doxorubicin hydrochloride can be partially deprotonated in buffer and in the vesicle membrane; therefore, Doxorubicin should be in the basic form when incapsulated into vesicle membrane. His-tagged proteins were added during hydration step at a concentration of 5 μM together with 20 mM $MgCl_2$ and 200 μM $NiCl_2$. Samples were stable for days but were usually imaged on the same day. For imaging, samples were diluted 1:30 in PBS. Due to issues with liposome stability and clumping we chose to dilute samples rather than applying them to a spin column to remove excess dye or drug. DNA was always added in a subsequent step, after vesicles were already formed, at a concentration of 100 nM.

Fluorescence Microscopy. For all imaging experiments, samples were pipetted into custom gasket imaging chambers and imaged in brightfield and using 488 and 561 nm laser illumination on an inverted confocal microscope (Olympus IX81) containing a spinning disk head (Yokogawa ×1). Images were acquired using a 100× 1.4 NA oil objective, an EM-CCD (Andor iXon3) camera, and MetaMorph acquisition software. Images were collected at identical laser intensities and camera gain and exposed for the same period of time.

Image Analysis. Images were analyzed manually in ImageJ. We masked the lamellar region and an internal region and calculated either the concentration of fluorescent signal inside the vesicle or the summed pixel intensity in the vesicle boundary. Internal and total loaded concentrations were calculated by taking the average intensity from the appropriate masked region and subtracting fluorescent background from outside of the vesicle and calibrating it to known concentration standards. Boundary intensity was calculated by subtracting integrating pixel intensity between the outer and inner masked regions. Most measurements included at least 20 vesicles. Concentration of dye or drug loaded was estimated using a standard curve for fluorescence.

Analysis of Statistical Significance. To falsify the hypothesis that the differences between 2 sets of data could be explained by chance, we performed 2-tailed, unpaired Fisher *t* tests, making binary comparisons between datasets using Excel and Prism. Sample number $n > 15$ was acquired and analyzed for each set of data. We report *P* values as $*P < 0.05$, $**P < 0.01$, and $***P < 0.001$; ns indicates nonsignificant. A *P* value less than 0.05 is considered to be significant.

ACKNOWLEDGMENTS. We thank Grishchuk laboratory (University of Pennsylvania) for a gift of His-SNAP expression vector and protein. We thank the Cell and Developmental Biology Microscopy Core (Perelman School of Medicine, University of Pennsylvania) for the support of imaging. This work was supported by National Science Foundation Grants DMR-1066116, DMR-1807127, and DMR-1120901; the P. Roy Vagelos Chair at the University of Pennsylvania (all to V.P.); DMR-1720530 (to M.C.G. and V.P.); the Alexander von Humboldt Foundation (to N.Y.K. and V.P.); Burroughs Wellcome Fund (to M.C.G.); Sheikh Saqr Research Foundation (to M.L.K.); and the European Union's Horizon 2020 research and innovation programme under the Marie Skłodowska-Curie Grant Agreement 642687 (to I.B.) and H2020-NMBP-TR-IND-2018, EVPRO (Development of Extracellular Vesicles loaded hydrogel coatings with immunomodulatory activity for Promoted Regenerative Osseointegration of revision endoprosthesis) grant 814495-2 (to C.R.-E. and N.Y.K.).

1. S. Rasmussen *et al.*, *Protocells: Bridging Nonliving and Living Matter* (The MIT Press, 2008), 10.7551/mitpress/9780262182683.001.0001.
2. Y. Sakuma, M. Imai, From vesicles to protocells: The roles of amphiphilic molecules. *Life (Basel)* **5**, 651–675 (2015).
3. B. Thaa, I. Levental, A. Herrmann, M. Veit, Intrinsic membrane association of the cytoplasmic tail of influenza virus M2 protein and lateral membrane sorting regulated by cholesterol binding and palmitoylation. *Biochem. J.* **437**, 389–397 (2011).
4. M. M. Hanczyc, J. W. Szostak, Replicating vesicles as models of primitive cell growth and division. *Curr. Opin. Chem. Biol.* **8**, 660–664 (2004).
5. S. S. Mansy, Protocells: Non-living predators. *Nat. Chem.* **9**, 107–108 (2017).
6. R. Lentini *et al.*, Integrating artificial with natural cells to translate chemical messages that direct E. coli behaviour. *Nat. Commun.* **5**, 4012 (2014).
7. C. G. Palivan *et al.*, Bioinspired polymer vesicles and membranes for biological and medical applications. *Chem. Soc. Rev.* **45**, 377–411 (2016).
8. A. Najer *et al.*, An amphiphilic graft copolymer-based nanoparticle platform for reduction-responsive anticancer and antimalarial drug delivery. *Nanoscale* **8**, 14858–14869 (2016).
9. D. Lingwood, K. Simons, Lipid rafts as a membrane-organizing principle. *Science* **327**, 46–50 (2010).
10. J. J. Amazon, S. L. Goh, G. W. Feigenson, Competition between line tension and curvature stabilizes modulated phase patterns on the surface of giant unilamellar vesicles: A simulation study. *Phys. Rev. E Stat. Nonlin. Soft Matter Phys.* **87**, 022708 (2013).
11. S. S. Mansy *et al.*, Template-directed synthesis of a genetic polymer in a model protocell. *Nature* **454**, 122–125 (2008).
12. P. Schwille *et al.*, MaxSynBio: Avenues towards creating cells from the bottom up. *Angew. Chem. Int. Ed. Engl.* **57**, 13382–13392 (2018).
13. R. J. Brea, M. D. Hardy, N. K. Devaraj, Towards self-assembled hybrid artificial cells: Novel bottom-up approaches to functional synthetic membranes. *Chemistry* **21**, 12564–12570 (2015).
14. S. L. Goh, J. J. Amazon, G. W. Feigenson, Toward a better raft model: Modulated phases in the four-component bilayer, DSPC/DOPC/POPC/CHOL. *Biophys. J.* **104**, 853–862 (2013).
15. R. Lentini, N. Yeh Martín, S. S. Mansy, Communicating artificial cells. *Curr. Opin. Chem. Biol.* **34**, 53–61 (2016).
16. S. Fujii, T. Matsuura, T. Sunami, Y. Kazuta, T. Yomo, In vitro evolution of α-hemolysin using a liposome display. *Proc. Natl. Acad. Sci. U.S.A.* **110**, 16796–16801 (2013).
17. K. Ikari *et al.*, Dynamics of fatty acid vesicles in response to pH stimuli. *Soft Matter* **11**, 6327–6334 (2015).
18. T. M. Allen, P. R. Cullis, Drug delivery systems: Entering the mainstream. *Science* **303**, 1818–1822 (2004).
19. B. M. Discher *et al.*, Polymersomes: Tough vesicles made from diblock copolymers. *Science* **284**, 1143–1146 (1999).
20. D. E. Discher *et al.*, Emerging applications of polymersomes in delivery: From molecular dynamics to shrinkage of tumors. *Prog. Polym. Sci.* **32**, 838–857 (2007).
21. S. E. Sherman, Q. Xiao, V. Percec, Mimicking complex biological membranes and their programmable glycan ligands with dendrimersomes and glycodendrimersomes. *Chem. Rev.* **117**, 6538–6631 (2017).
22. V. Percec *et al.*, Self-assembly of Janus dendrimers into uniform dendrimersomes and other complex architectures. *Science* **328**, 1009–1014 (2010).
23. M. Peterca, V. Percec, P. Leowanawat, A. Bertin, Predicting the size and properties of dendrimersomes from the lamellar structure of their amphiphilic Janus dendrimers. *J. Am. Chem. Soc.* **133**, 20507–20520 (2011).
24. Q. Xiao *et al.*, Bioactive cell-like hybrids coassembled from (glyco)dendrimersomes with bacterial membranes. *Proc. Natl. Acad. Sci. U.S.A.* **113**, E1134–E1141 (2016).
25. S. S. Yadavalli *et al.*, Bioactive cell-like hybrids from dendrimersomes with a human cell membrane and its components. *Proc. Natl. Acad. Sci. U.S.A.* **116**, 744–752 (2019).
26. S. Zhang *et al.*, Self-assembly of amphiphilic Janus dendrimers into uniform onion-like dendrimersomes with predictable size and number of bilayers. *Proc. Natl. Acad. Sci. U.S.A.* **111**, 9058–9063 (2014).
27. D. Boal, *Mechanics of the Cell* (Cambridge University Press, 2012).
28. V. Percec *et al.*, Modular synthesis of amphiphilic Janus glycodendrimers and their self-assembly into glycodendrimersomes and other complex architectures with bioactivity to biomedically relevant lectins. *J. Am. Chem. Soc.* **135**, 9055–9077 (2013).
29. S. Zhang *et al.*, Mimicking biological membranes with programmable glycan ligands self-assembled from amphiphilic Janus glycodendrimers. *Angew. Chem. Int. Ed. Engl.* **53**, 10899–10903 (2014).
30. S. Zhang *et al.*, Glycodendrimersomes from sequence-defined Janus glycodendrimers reveal high activity and sensor capacity for the agglutination by natural variants of human lectins. *J. Am. Chem. Soc.* **137**, 13334–13344 (2015).
31. Q. Xiao *et al.*, Onion-like glycodendrimersomes from sequence-defined Janus glycodendrimers and influence of architecture on reactivity to a lectin. *Proc. Natl. Acad. Sci. U.S.A.* **113**, 1162–1167 (2016).
32. A.-K. Ludwig *et al.*, Design-functionality relationships for adhesion/growth-regulatory galectins. *Proc. Natl. Acad. Sci. U.S.A.* **116**, 2837–2842 (2019).
33. Q. Xiao *et al.*, Why do membranes of some unhealthy cells adopt a cubic architecture? *ACS Cent. Sci.* **2**, 943–953 (2016).
34. C. Rodriguez-Emmenegger *et al.*, Encoding biological recognition in a bicomponent cell-membrane mimic. *Proc. Natl. Acad. Sci. U.S.A.* **116**, 5376–5382 (2019).
35. V. Percec *et al.*, Self-assembly of amphiphilic dendritic dipeptides into helical pores. *Nature* **430**, 764–768 (2004).
36. M. S. Kaucher *et al.*, Selective transport of water mediated by porous dendritic dipeptides. *J. Am. Chem. Soc.* **129**, 11698–11699 (2007).
37. Q. Xiao *et al.*, Self-sorting and coassembly of fluorinated, hydrogenated, and hybrid Janus dendrimers into dendrimersomes. *J. Am. Chem. Soc.* **138**, 12655–12663 (2016).
38. Q. Xiao *et al.*, Janus dendrimersomes coassembled from fluorinated, hydrogenated, and hybrid Janus dendrimers as models for cell fusion and fission. *Proc. Natl. Acad. Sci. U.S.A.* **114**, E7045–E7053 (2017).
39. I. Buzzacchera *et al.*, Screening libraries of amphiphilic Janus dendrimers based on natural phenolic acids to discover monodisperse unilamellar dendrimersomes. *Biomacromolecules* **20**, 712–727 (2019).
40. S. E. Wilner *et al.*, Dendrimersomes exhibit lamellar-to-sponge phase transitions. *Langmuir* **34**, 5527–5534 (2018).
41. S. Sur, A. C. Fries, K. W. Kinzler, S. Zhou, B. Vogelstein, Remote loading of preencapsulated drugs into stealth liposomes. *Proc. Natl. Acad. Sci. U.S.A.* **111**, 2283–2288 (2014).
42. Y. Malam, M. Loizidou, A. M. Seifalian, Liposomes and nanoparticles: Nanosized vehicles for drug delivery in cancer. *Trends Pharmacol. Sci.* **30**, 592–599 (2009).
43. U. Bulbake, S. Doppalapudi, N. Kommineni, W. Khan, Liposomal formulations in clinical ase: An updated review. *Pharmaceutics* **9**, 12 (2017).

44. A. Gabizon, H. Shmeeda, Y. Barenholz, Pharmacokinetics of pegylated liposomal Doxorubicin: Review of animal and human studies. *Clin. Pharmacokinet.* **42**, 419–436 (2003).
45. L. R. Paborsky, K. E. Dunn, C. S. Gibbs, J. P. Dougherty, A nickel chelate microtiter plate assay for six histidine-containing proteins. *Anal. Biochem.* **234**, 60–65 (1996).
46. B. C. Roy, S. Mallik, Synthesis of new polymerizable metal-chelating lipids. *J. Org. Chem.* **64**, 2969–2974 (1999).
47. Y. S. Casadio, D. H. Brown, T. V. Chirila, H.-B. Kraatz, M. V. Baker, Biodegradation of poly(2-hydroxyethyl methacrylate) (PHEMA) and poly(2-hydroxyethyl methacrylate)-co-[poly(ethylene glycol) methyl ether methacrylate] hydrogels containing peptide-based cross-linking agents. *Biomacromolecules* **11**, 2949–2959 (2010).
48. L. Kai, P. Schwille, Cell-free protein synthesis and its perspectives for assembling cells from the bottom-up. *Adv. Biosys.* **3**, 1800322 (2019).
49. R. Lipowsky, Domains and rafts in membranes—Hidden dimensions of selforganization. *J. Biol. Phys.* **28**, 195–210 (2002).
50. E. Jiménez *et al*., Generation of lung adenocarcinoma DNA aptamers for cancer studies. *PLoS One* **7**, e46222 (2012).
51. M. Vidic *et al*., In silico selection approach to develop DNA aptamers for a stem-like cell subpopulation of non-small lung cancer adenocarcinoma cell line A549. *Radiol. Oncol.* **52**, 152–159 (2018).
52. N. Arai, K. Yasuoka, X. C. Zeng, Self-assembly of Janus oligomers into onion-like vesicles with layer-by-layer water discharging capability: A minimalist model. *ACS Nano* **10**, 8026–8037 (2016).
53. M. A. Oberli *et al*., Lipid nanoparticle assisted mRNA delivery for potent cancer immunotherapy. *Nano Lett.* **17**, 1326–1335 (2017).
54. O. C. Farokhzad, R. Langer, Impact of nanotechnology on drug delivery. *ACS Nano* **3**, 16–20 (2009).
55. T. Wei *et al*., Anticancer drug nanomicelles formed by self-assembling amphiphilic dendrimer to combat cancer drug resistance. *Proc. Natl. Acad. Sci. U.S.A.* **112**, 2978–2983 (2015).